Heliyon 10 (2024) e26797

Contents lists available at ScienceDirect

Heliyon

journal homepage: www.cell.com/heliyon

Research article

Sensitivity analysis and thermodynamic evaluation of a combined cooling, heating and power system utilizing exhaust gases of smelting furnace

Sina Hassanlue [a], Azfarizal Mukhtar [b,**], Ahmad Shah Hizam Md Yasir [c], Sayed M. Eldin [d], Mohammad A. Nazari [e,f,g], Mohammad Hossein Ahmadi [h], Mohsen Sharifpur [i,j,k,*]

[a] Faculty of Aerospace Engineering, Amirkabir University of Technology, Tehran, Iran
[b] Institute of Sustainable Energy, Putrajaya Campus, Universiti Tenaga Nasional, Jalan IKRAM-UNITEN, 43000, Kajang, Malaysia
[c] Faculty of Resilience, Rabdan Academy, 65, Al Inshirah, Al Sa'adah, Abu Dhabi, 22401, PO Box: 114646, Abu Dhabi, United Arab Emirates
[d] Center of Research, Faculty of Engineering, Future University in Egypt New, Cairo, 11835, Egypt
[e] Institute of Research and Development, Duy Tan University, Da Nang, Viet Nam
[f] School of Engineering & Technology, Duy Tan University, Da Nang, Viet Nam
[g] Research and Development Cell, Lovely Professional University, India
[h] Faculty of Mechanical Engineering, Shahrood University of Technology, Shahrood, Iran
[i] Department of Mechanical and Aeronautical Engineering, University of Pretoria, Pretoria, 0002, South Africa
[j] School of Mechanical, Industrial and Aeronautical Engineering, University of the Witwatersrand, Private Bag 3, Wits 2050, South Africa
[k] Department of Medical Research, China Medical University Hospital, China Medical University, Taichung, Taiwan

ARTICLE INFO

Keywords:
Heat recovery
Smelting furnace
Absorption chiller
Supercritical CO2
CCHP system

ABSTRACT

Exhaust gases from the smelting furnace have high temperature and mass flow rate, and there is huge potential to use them for energy-related purposes such as electricity generation, cooling and heating. Utilization of the gases for energy-related purposes would lead to fuel savings and emissions reduction. To use this potential, it is necessary to design proper systems and cycles and apply a heat recovery unit. Several technologies are useable for heat recovery depending on the characteristics of exhaust gases, such as their mass flow rate, temperature and compositions. Due to the higher potential of combined heating, cooling and power (CCHP) generation systems compared with the systems with a single output, a CCHP is designed and investigated in the present study by consideration of the specifications of the exhaust gases. The applied system in this study comprises a Supercritical CO_2 (SCO_2) cycle, heat exchanger and single-stage absorption chiller for simultaneous heating, cooling and power production. Engineering Equation Solver (EES) is employed to model the proposed system by considering the properties of the flows and characteristics of the components. To get deep insight into the effective parameters on the outputs of the designed system, the impact of three factors, namely the mass flow rate of the gases, the effectiveness of heat exchanger and temperature of exhaust gases, are analyzed and investigated by the implementation of sensitivity analysis. As one of the main conclusions, it is found that an

* Corresponding author. Department of Mechanical and Aeronautical Engineering, University of Pretoria, Pretoria, 0002, South Africa .
** Corresponding author.
E-mail addresses: Sina.hassanlue@aut.ac.ir (S. Hassanlue), azfarizal@uniten.edu.my (A. Mukhtar), ayasir@ra.ac.ae (A.S.H.M. Yasir), sayed.eldin22@fue.edu.eg (S.M. Eldin), mohammadalhuyinazari@duytan.edu.vn (M. A. Nazari), mohammadhosein.ahmadi@gmail.com (M.H. Ahmadi), mohsen.sharifpur@up.ac.za (M. Sharifpur).

https://doi.org/10.1016/j.heliyon.2024.e26797
Received 11 May 2023; Received in revised form 22 January 2024; Accepted 20 February 2024
Available online 28 February 2024

increment in the mass flow rate of exhaust gases from 30 kg/s to 70 kg/s causes augmentation in the power generation from 2037 kW to 4754 kW. Furthermore, exergy analysis is carried out, and it is found that an increase in the temperature or mass flow rate of exhaust gases or a decrease in the effectiveness of heat exchangers would lead to decrement in the exergy efficiency of the system. According to the performed sensitivity analysis, the mass flow rate of exhaust gases has the most remarkable influence on the heating and cycle-generated power among the considered factors.

Abbreviations	
AC	Absorption Chiller
ARC	Absorption Refrigeration Cycle
CCHP	Combined Cooling, Heating and Power
CPR	Compressor Pressure Ratio
COP	Coefficient of Performance
ED	Exergy Destruction
EES	Engineering Equation Solver
EG	Exhaust Gases
HRU	Heat Recovery Unit
MFR	Mass Flow Rate
OFC	Organic Flash Cycle
ORC	Organic Rankine Cycle
S–CO2	Supercritical CO2
ST	Solar Thermal
WHR	Waste Heat Recovery
WTE	Waste to Energy

1. Introduction

Augmentation in the emission of greenhouse gases like NOx, CO_2 and CO, fluctuations in the fossil fuels prices and restrictions in the sources of conventional fossil fuels have necessitated the development of alternative systems and energy sources [1–3]. Efficiency improvement of the systems by applying some approaches such as performance optimization and, utilizing the waste heats and making use of clean energy technologies based on the renewable energy sources are among the most practical solutions for the above-mentioned issues. Heat recovery can be implemented from the waste heat of various systems, namely Exhaust Gases (EG) of power plants [4], cars [5], fuel cells [6] and different industries [7,8]. Supplied energy by Waste Heat Recovery (WHR) systems are applicable for various purposes like heating, cooling and power production. For instance, Wang et al. [9] applied low-pressure economizer for WHR from exhaust flue gases in a power plant. They reported some benefits for this system, including standard coal equivalent saving, water saving and decrement in CO_2 emission. Orr and Akbarzadeh [10] investigated applications of thermoelectric generators for power generation from the WHR system and reported that by using a thermoelectric generator, it would be possible to produce 1.4 kW electricity from the EG of a car in a condition of engine production of 150 kW. Xu et al. [11]analyzed a WHR system of a power plant by using serial absorption heat pumps on a large scale. It was pointed out that a heating capacity of 63.57 MW and Coefficient of Performance (COP) of 1.77 were obtainable by applying one serial absorption heat pump in case of inlet/outlet temperature of waste heat equal to 34.63/28.33 $^{\circ}C$ and inlet/outlet return water temperature of 45.94/81.34 $^{\circ}C$.

There is significant potential for EG from smelting furnaces to utilize their waste heat for different purposes. Different scholars have implemented studies on the WHR from various industries [12]. In a study by Naeimi et al. [13], two scenarios were analyzed for power generation by heat recovery from a cement factory. In the first case, just one heat recovery boiler was applied. In this case, total mixed gas goes to the boiler before going to the grid cooler and preheater. In the second configuration, there was a vapor mixture that went to the steam turbine. They reported that the efficiency of the first and second configurations was 23.5% and 22.2%, respectively. In another work by Chen et al. [14], a new WHR system for cement plant was introduced and analyzed. WHR was integrated with a coal-fired power plant regeneration process in this configuration. Their findings showed that the proposed WHR system can generate 6.75 MW more net power than the conventional one. Gomaa et al. [15] investigated the potential of WHR from a cement factory by making use of a thermoelectric generator. In their work, some thermoelectric generators were installed on a secondary coaxial shell that was separated from the shell of the kiln and two cooling approaches, namely forced air and active water, were applied. They noted that using active water cooling induces a 4.4% enhancement in the power of thermoelectric generators compared with forced air cooling. Furthermore, an economic analysis was implemented, and it revealed that the payback periods of the active water cooling and forced air approaches were 16 and 9 months, respectively. Aside from cement factory, heat recovery has been applied for other industries. For instance, aluminum industry is one of the sectors with high potential for heat recovery. According to a review article on this industry [16], employment of waste heat recovery technology is one of the approaches for decreasing energy consumption and decrementing the environmental effects of emissions.

There are different cycles for power generation by use of thermal energy; however, Brayton cycles with supercritical fluids are one of the most appropriate types for the aim of the present work, which is electricity generation from the recovered heat of melting

furnace exhaust. The supercritical Brayton Cycle (SCBC) is among the promising cycles applicable for power generation regarding the compactness of its configuration and proper thermal efficiency at relatively low temperatures at the inlet of the turbine (450-750 $^{\circ}C$) [17]. Supercritical CO_2 (S–CO_2) is one of the most conventional working fluids useable in SCBCs. Various studies have investigated different aspects of SCBC with CO_2 as the operating fluid. A study by Chen et al. [18] proposed a hybrid system by adding S–CO_2 cycle. In the proposed system, the S–CO_2 cycle gains thermal energy from the Waste-to-Energy (WTE) boiler superheater and the produced saturated steam by the boiler of WTE was applied as the thermal source for the coal power plant feedwater. The system function was compared with the conventional separate scheme. Their findings revealed that the efficiency of WTE was augmented by 8.34%. In another study [19], the potential of two novel layouts for the S–CO2 cycle, namely single and dual flow split with dual expansion for waste heat recovery, was compared with the traditional single recompression and recuperated layouts. It was observed that the dual flow split and dual expansion has the best function among the considered layouts. Olumayegun and Wang [20] carried out a study on the S–CO_2 cycle dynamic modelling and control utilizing waste heat from industrial processes. Results of the work indicated that the single recuperator recompression S–CO_2 cycle thermal efficiency is around 33%. System stable operation can be obtained by making use of a throttle valve and cooling water control to keep the outlet condition of the precooler constant. Wang et al. [21] implemented a parametric optimization design for the S–CO2 cycle by applying a neural network and genetic algorithm. It was reported that key thermodynamic factors like turbine inlet pressure and temperature and ambient temperature have a remarkable influence on the performance of the system and Exergy Destruction (ED) in each unit. S–CO_2 cycles could be coupled with clean energy technologies like solar systems for power generation. Some studies have investigated these types of S–CO_2 cycles, utilizing renewable energy sources. In a study by Novales et al. [22], sensitivity analysis was carried out on the partial cooling and recompression cycles for concentrating solar power, and it was found that the recompression cycle efficiency is remarkably more sensitive than the other one. Sun et al. [23] implemented a study on parametrized analysis and optimization of the S–CO_2 cycle integrated with parabolic trough collectors. The findings recommended that a simple recuperation cycle scheme shows a more appropriate function in comparison with the intercooling scheme and recompression cycle scheme in terms of cost; however, the advantage in specific work of recompression and intercooling cycle layouts is not obvious.

Combined Cooling, Heating and Power (CCHP) systems have captured attention in recent years regarding their high energy efficiency and lower emissions of greenhouse gases in comparison with conventional systems with the ability to produce just power. These systems are similar to combined heating and power systems with additional components for cooling production [24]. Generally, CCHP systems are applied in thermal power plants utilizing fossil fuels [25]; however, using other energy sources in CCHP systems is possible. Different configurations have been proposed to have CCHP systems depending on the available sources and required outputs. In a study by Ai et al. [26], a CCHP that was integrated with a regenerative organic flash cycle was analyzed. Their study designed a novel configuration by coupling a regenerative organic flash cycle (OFC) and solar thermal (ST) input system. The CCHP-ST-OFC function was assessed and compared with a conventional CCHP and CCHP-ST-Organic Rankine Cycle (ORC). They reported that heat provisions and electricity were 19.3 kW and 4.7 kW higher than the CCHP-ST-ORC system. OFC subsystem electricity was 47% higher than the ORC system. In a study by Wang et al. [27], a CCHP system composed of S–CO_2 cycle, gas turbine, Absorption Refrigeration Cycle (ARC), steam generator, ORC and additional thermoelectric generator was analyzed. It was noted that the employment of a thermoelectric generator induces a 0.3% increment in the thermal efficiency under design conditions; however, it leads to a 0.45 $/h higher cost rate and around 19 kt $CO_{2\ eq}$ larger emissions. In another work [28], a CCHP system composed of a regenerative S–CO_2 cycle, ORC, gas turbine cycle and ARC for waste heat recovery from a gas turbine was investigated. Findings revealed that overall exergoeconomic factor of the system after exergoeconomic aspect optimization is 20.17%. The highest ED rate in the investigated system was the component combustion chamber; however, the gas turbine cycle has the highest total ED. Wang et al. [29] investigated a CCHP system composed of a regenerative gas turbine cycle as the runner system and ejector refrigeration cycle, and Kalina cycle as the companion components. Thermodynamic modeling demonstrated that approximately 75% of total ED is associated with regenerative gas turbine cycle.

Till now, the majority of the studies on heat recovery from industries have focused on power generation by making use of different cycles such as ORC [30] and Kalina [31], and some others have investigated power generation by use of some components like thermoelectric generator [15]. Due to the better performance of CCHP systems in terms of overall efficiency and products, it would be beneficial to develop these systems to utilize recovered heat from EG of the smelting furnaces. The generated electricity can be connected to the grid or applied for the facilities' power requirement. The produced heating and cooling are applicable in residential facilities in the vicinity of the location of the smelting furnace. To have a suitable system with appropriate outputs, it is crucial to use proper configuration and components. In this work, a CCHP system composed of Absorption Chiller (AC), heat exchanger and S–CO_2 cycle utilizing EG of a smelting furnace is thermodynamically investigated. Due to the involvement of various factors in the overall performance and outputs of the designed systems, assessing some of the most important parameters is beneficial. In this regard, the impacts of different factors like temperature and flow rate of EG and heat exchanger effectiveness on the proposed system's output are evaluated and analyzed. Furthermore, sensitivity analysis is implemented to find the importance level of the mentioned factors. The most important hypotheses and aims of the present work could be outlined as follows.

- If it is technically feasible to apply EG from a smelting furnace to produce power, heating and cooling.
- How the outputs of the designed system would be affected by variations in the temperature and Mass Flow Rate (MFR) of EG and the effectiveness of the applied heat exchanger?
- To what extent do each of the mentioned factors affect the efficiency and outputs of the system?
- What are each product's shares in the system's total outputs?
- How would the system's exergy efficiency be affected by variations in the considered variables?

Details of the proposed system, assumptions and modeling process are provided in the following sections.

2. Proposed system and applied equations

This study investigates a CCHP system utilizing EG of a smelting furnace. Schematic of the proposed configuration is illustrated in Fig. 1. There are different cycles for power generation by waste heat recovery. S–CO_2 cycles are useable for higher temperatures of waste heat sources compared to ORC, i.g. temperatures higher than 400 [32,33]. In Fig. 2, a comparison of various working ranges of heat to power systems based on bottoming thermodynamic cycles for WHR is provided. Similarly, it is reported that Kalina cycle more believable application is limited to heat sources with medium-low temperatures, typically the highest temperature of 300 °C-400 °C in condition of heat recovery. Since the aim of the present study is heat recovery from smelting furnace EG with ta temperature of higher than 450 °C, the S–CO2 cycle is applied for the power generation section of the system. In this layout, the EG, with properties mentioned in Table 1, enter the primary heat exchanger to supply the thermal energy of an S–CO_2 cycle with precooler and recuperator. Afterwards, it enters the 2nd heat exchanger to provide hot water. In this heat exchanger, cold water receives heat from the EG and its temperature increases. Subsequently, the EG go through ta single effect AC's generator (desorber) Equations used for the modeling of the systems are provided separately in this section. It should be noted that the range of temperature of gases ais considered based on another study, which has been assumed equal to 550 °C [34], while it has varied around this value in this work to investigate its effect. The MFR of EG depends on the furnace's capacity and dimensions. Here, we considered MFR in the range of 30 kg/s-50 kg/s to have enough energy input for the generation of different products.

2.1. SCO_2 cycle

The considered S–CO_2 cycle in this study is composed of compressor, turbine, primary heat exchanger, recuperator and precooler. Applied work by the compressor is determined based on the total enthalpy (h_0) and the efficiency of the compressor (η_{Comp}) by using Equation (1) as follows:

$$W_{comp} = \frac{\acute{h}_{02} - h_{01}}{\eta_{Comp}} \tag{1}$$

where the compressor efficiency is assumed to be equal to 0.80 since it has been between 75% [36] and 85% [37] in the previous works. h_{01} refers to the enthalpy of CO_2 by considering total temperature and total pressure as follows, Equations (2) and (3), respectively.

$$h_{01} = h\{CO_2, T = T_{01},\ P = P_{01}\} \tag{2}$$

$$\acute{h}_{02} = h\{CO_2, s = \acute{s}_{02}, P = P_{02}\} \tag{3}$$

where $\acute{s}_{02}$ is the entropy of fluid obtained in an isentropic process and is equal to s_{01}. The total pressure at point 2 (P_{02}) is determined based on the Compressor Pressure Ratio (CPR) according to Equation (4) as follows:

$$P_{02} = CPR.P_{01} \tag{4}$$

To determine the enthalpy, temperature and entropy of the stream at point 2, Equations (5)–(7) are applied:

$$h_{02} = h_{01} + W_{comp} \tag{5}$$

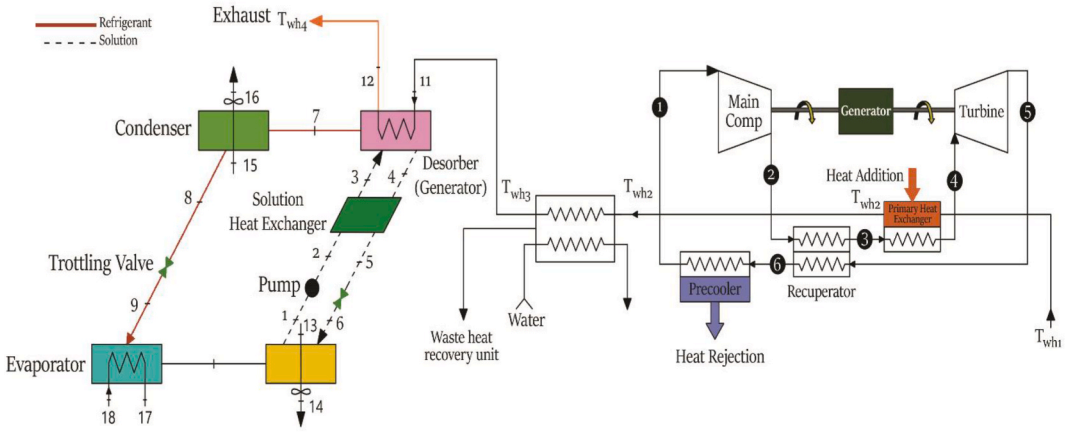

Fig. 1. Schematic of CCHP system utilizing EG of smelting furnace.

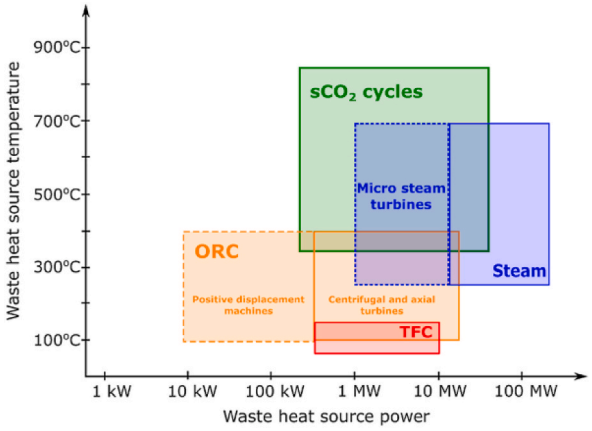

Fig. 2. Comparison of various working ranges of heat to power conversion systems [35].

Table 1
Properties of the EG from a smelting furnace.

Mass Flow Rate (kg/s)	30, 40, 50, 60 and 70
Cp (kj/kg.K)	0.96
T_0 (°C)	490, 520, 550, 580 and 610
P_0 (Pa)	101325

$$T_{02} = T\{CO_2\ h = h_{02}, P = P_{02}\} \tag{6}$$

$$s_{02} = s\{CO_2, T = T_{02}, P = P_{02}\} \tag{7}$$

Total enthalpy and temperature at the outlet of the recuperator section are obtained according to Equations (8) and (9), respectively.

$$h_{03} = \varepsilon.(h_{05} - h\{CO_2, T = T_{02}, P = P_{05}\}) + h_{02} \tag{8}$$

$$T_{03} = T\{CO_2, h = h_{03}, P = P_{03}\} \tag{9}$$

In the primary heat exchanger, Equations (10)–(12) can be written based on energy conversion in this component of the system:

$$\dot{m}_{CO_2} = \frac{C_{P,exh}.\left(T_{exh,in} - T_{exh,out}\right)}{h_{04} - h_{03}} \tag{10}$$

$$h_{06} = h_{05} - (h_{03} - h_{02}) \tag{11}$$

$$T_{06} = T\{CO_2, h = h_{06}, P = P_{06}\} \tag{12}$$

Generated work in the turbine can be determined by applying Equation (13):

$$W_{Turb} = (h_{04} - \acute{h}_{05}).\eta_{Turb} \tag{13}$$

where η_{Turb} is assumed equal to 0.85 since it has been considered in range of 80% [36] to 90% [37] in the previous studies and $\acute{h}_{05}$ is determined by using Equation (14).

$$\acute{h}_{05} = h\{CO_2, s = \acute{s}_{05}, P = P_{05}\} \tag{14}$$

In the abovementioned equation, $\acute{s}_{05} = s_{04}$. Enthalpy, temperature and entropy at point 5 are determined by applying Equations (15)–(17).

$$h_{05} = h_{04} - W_{Turb} \tag{15}$$

$$T_{05} = T\{CO_2, h = h_{05}, P = P_{05}\} \tag{16}$$

$$s_{05} = s\{CO_2, h = h_{05}, P = P_{05}\} \tag{17}$$

Equations (19)–(26) are used to evaluate the cycle and determine its efficiency:

$$\dot{Q}_{Heater} = \dot{m}_{CO_2}.(h_{04} - h_{03}) \tag{19}$$

$$\dot{Q}_{Recuperator} = \dot{m}_{CO_2}.(h_{03} - h_{02}) \tag{20}$$

$$\dot{Q}_{Precooler} = \dot{m}_{CO_2}.(h_{06} - h_{01}) \tag{21}$$

$$\dot{W}_{Comp} = \dot{m}_{CO_2}.(h_{06} - h_{01}) \tag{22}$$

$$\dot{W}_{Turb} = \dot{m}_{CO_2}.(h_{04} - h_{05}) \tag{23}$$

$$Power = \eta_{Gen}\left(\eta_{Mech}.\ \dot{W}_{Turb} - \dot{W}_{Comp}\right) \tag{24}$$

$$\dot{W}_{net} = \eta_{Mech}.\dot{W}_{Turb} - \dot{W}_{Comp} \tag{25}$$

$$\eta_{sCO_2} = \frac{\dot{W}_{net}}{\dot{Q}_{Heater}} \tag{26}$$

where η_{Gen} and η_{Mech} are generator efficiency and mechanical efficiency which are assumed equal to 0.90 and 0.99, respectively.

2.2. Single effect absorption chiller

In this subsection, equations applied for the determination of the AC system performance are represented. The mass balance in the desorber section of AC system can be written as Equation (27).

$$\dot{m}_3 = \dot{m}_4 + \dot{m}_7 \tag{27}$$

Equations (28) and (29) represent the relationships between the MFR and quality of the streams.

$$\dot{m}_3 x_3 = \dot{m}_4 x_4 \tag{28}$$

$$\dot{m}_3(1 - x_3) = \dot{m}_4(1 - x_4) + \dot{m}_7 \tag{29}$$

For other points of the cycle, mass balance is determined by using the relationships provided in Equation (30).

$$x_8 = x_7\ x_9 = x_8\ x_{10} = x_9\ x_2 = x_1\ x_6 = x_5\ x_5 = x_4\ x_3 = x_2\ \dot{m}_8 = \dot{m}_7\ \dot{m}_9 = \dot{m}_8\ \dot{m}_{10} = \dot{m}_9\ \dot{m}_2 = \dot{m}_1\ \dot{m}_6 = \dot{m}_5\ \dot{m}_5 = \dot{m}_4\ \dot{m}_3 = \dot{m}_2 \tag{30}$$

In the above equation, x refers to the quality of the stream in each point. In the absorber section, mass balance can be written according to Equation (31).

$$\dot{m}_1 = \dot{m}_{10} + \dot{m}_6 \tag{31}$$

Where Equation (32) represents the relationship between the MFR and quality of the stream.

$$\dot{m}_4 x_4 = \dot{m}_3 x_3 \tag{32}$$

Temperatures at points 8 and 10 are determined as follows:

$$T_8 = T_{Sat,Liquid}(P_H) \tag{33}$$

$$T_{10} = T_{Sat,Vapor}(P_L) \tag{34}$$

where P_H and P_L are high and low pressure of the AC cycle, respectively.

At points 1 and 4, temperature is calculated by use of Equations (35) and (36), respectively.

$$T_1 = T_{Sat}(P_L, x_1) \tag{35}$$

$$T_4 = T_{Sat}(P_H, x_4) \tag{36}$$

Rates of heat transfer in the absorber, desorber, evaporator, condenser and solution heat exchanger are determined by using Equations (37)–(42), respectively.

$$\dot{Q}_{Absorber} = \dot{m}_1 h_1 + \dot{m}_{10} h_{10} + \dot{m}_6 h_6 \tag{37}$$

$$\dot{Q}_{Desorber} = \dot{m}_4 h_4 + \dot{m}_7 h_7 + \dot{m}_3 h_3 \tag{38}$$

$$\dot{Q}_{Evaporator} = \dot{m}_{10}h_{10} - \dot{m}_9 h_9 \tag{39}$$

$$\dot{Q}_{Condenser} = -\dot{m}_8 h_8 + \dot{m}_7 h_7 \tag{40}$$

$$\dot{Q}_{CS} = \dot{m}_3 h_3 - \dot{m}_2 h_2 \tag{41}$$

$$\dot{Q}_{HS} = -\dot{m}_5 h_5 + \dot{m}_4 h_4 \tag{42}$$

where $h_9 = h_8$ and $h_6 = h_5$. In the pump of AC system, following equations can be used to determine enthalpy at the outlet of it.

$$h_2 = h_1 + (v_1 \Delta P)/\eta_p \tag{43}$$

where η_p is the pump efficiency and is assumed equal to 1 [38]. Enthalpy of the streams at different points are determined by using the relationships presented in Equation (44).

$$\begin{aligned} h_1 &= h(T_1, x_1)\ h_2 = h(T_2, x_2)\ h_3 = h(T_3, x_3)\ h_4 = h(T_4, x_4)\ h_5 = h(T_5, x_5)\ h_6 = h(T_6, x_6)\ h_7 = h(T_7, P_H)\ h_8 = h_{Sat,\text{Liquid}}(T_8)\ h_9 \\ &= h(P_L, Q_9)\ h_{10} = h_{Sat,\text{Vapor}}(T_{10}) \end{aligned} \tag{44}$$

Effectiveness of the heat exchanger and COP of the AC system are determined by use of Equations (45) and (46), respectively.

$$\varepsilon_{HX} = \frac{T_4 - T_5}{T_4 - T_2} \tag{45}$$

$$COP = \frac{\dot{Q}_e}{\dot{Q}_{Gen}} \tag{46}$$

2.3. Heat recovery unit (HRU)

Heat Recovery Unit (HRU) is another component of the investigated CCHP system. In this unit, a cold water stream with a temperature of about 20 °C enters the heat exchanger and receives heat from the hot gases leaving the S–CO_2 cycle. The MFR of cold water is regulated in a way to have water with an outlet temperature of 60 °C [ASHRAE] The applied equations for this component of the system are as follows.

$$\dot{Q}_{HRU} = \dot{m}_{exh} C_{p_{exh}} \left(T_{WH_2} - T_{WH_3}\right) \tag{47}$$

$$\dot{m}_{HotWater} = \dot{Q}_{HRU} \,/\, C_{p_{water}} (T_{HotWater} - T_{ColdWater}) \tag{48}$$

2.4. Pinch point

The location in which the temperature difference between cold and hot fluid is at its minimum value is referred to as the pinch point in the heat exchanger. In optimum design can assume that the hot side and cold side temperature difference is constant and equal to the pinch point temperature as represented in Equations (49) and (50).

$$T_{04} = T_{WH_1} - \Delta T_{Pinch} \tag{49}$$

$$T_{WH_2} = T_{03} + \Delta T_{Pinch} \tag{50}$$

In order to solve the equations, Engineering Equation Solver (EES) is applied.

2.5. Exergy analysis

In addition to energy, exergy efficiency of the system is determined for the proposed system. Equation (51) is applied for calculation of exergy efficiency as follows:

$$\eta_{ex,CCHP} = \frac{\dot{W}_{net} + \dot{ex}_{heating} + \dot{ex}_{cooling}}{\dot{ex}_{fuel}} \tag{51}$$

Equations (52) and (53) are used to calculate exergy products related to heating and cooling, respectively.

$$\dot{ex}_{heating} = \dot{m}_w \left((h_{out} - h_0) - T_0(s_{out} - s_0) - ((h_{in} - h_0) - T_0(s_{in} - s_0))\right) \tag{52}$$

$$\dot{ex}_{cooling} = \left(1 - \frac{T_0}{T_{cool}}\right) \dot{Q}_{cooling} \tag{53}$$

where T_0 is ambient temperature and cis considered equal to 25 °C. Subscript 0 refers to the dead state, which means ambient temperature and pressure. Exergy product is determined by using Equation (54) as follows:

$$ex_{fuel=}\dot{m}_{WH}\left(C_p \times (T_{Wh1} - T_{Wh4}) - T_0 C_p \ln\left(T_{Wh1}/T_{Wh4}\right)\right) \quad (54)$$

3. Hypothesis and assumptions

EG from the smelting furnace have high temperature and there is potential for power generation, heating and cooling by use of heat recovery systems. In this regard, the present study aims to evaluate feasibility of a CCHP system and assess the potential of EG for production of power, heating and cooling. Furthermore, we aim to assess the impact of some of the most important factors such as the MFR and temperature of EG and effectiveness of the heat exchanger used for heating production. Furthermore, exergy analysis would be considered to get deeper insight into the proposed system and its efficiency. In the base case of the present study, temperature of EG is considered 550 $°C$ according to Ref. [34]. The considered temperatures in the present work varies between the base case in range of 490–610 $°C$. MFR of the EG is dependent on the dimensions and capacity of furnace. We consider 50 kg/s as the base case for MFR of EG that can be generated form a large smelting furnace or more than one furnace with smaller scales. The assumptions for the considered AC cycle are as follows [39]:

$T_{Absorber} = 38°C$
$T_{Condenser} = 38°C$
$T_{Generator} = 120°C$
$T_{Evaporator} = 8°C$
$x_7 = 0$
$\dot{m}_{Refigerant} = 1kg/s$
$\varepsilon_{HE} = 0.70$
Pinch point = 30 °C

Where ε_{HE} is the effectiveness of the heat exchanger used in the AC cycle between absorber and desorber. The pinch point in the generator is assumed to be equal to 30°Cand pressure loss and heat loss in all components is assumed to be negligible. Other assumptions, such as the efficiency of the components in the power generation cycle, are presented in Table 2.

Flow properties in different points, according to the constraints and assumptions, are provided in Tables 3–5.

Table 2
Assumptions of the model for the power generation cycle.

T_{01}	**32**	**°C**
P_{01}	7.5	Mpa
CPR	3.5	–
Effectiveness	0.8	–
Compressor efficiency	0.8	–
Turbine efficiency	0.85	–
Generator efficiency	0.9	–
Mechanical efficiency	0.99	–
Pressure loss	–	–
Specific heat and exhaust gases	0.96	kJ/kg.K
Pinch point	20	°C

Table 3
Stream properties of AC cycle for exhaust MFR of 50 kg/s, effectiveness of 0.80 and exhaust temperature of 550 $°C$.

Point	T_0 [°C]	H_0 [kJ/kg]	Q (vapor quality)	X (mass fraction)	Mass Flow Rate [kg/s]
1	38	93.98	–	0.553	9.303
2	38	93.99	–	0.553	9.303
3	70.68	161	–	0.553	9.303
4	120	368.9	–	0.7413	8.303
5	62.6	279.1	–	0.7413	8.303
6	62.6	279.1	–	0.7413	8.303
7	72.06	2635	–	0	1
8	38	159.2	–	0	1
9		159.2	0.05058	0	1
10	8	2516	0	0	1

Table 4
Specifications of the stream in each point for S–CO_2 cycle for exhaust MFR of 50 kg/s, effectiveness of 0.80 and exhaust temperature of 550 °C.

Point	T_0 [K]	P_0 [Mpa]	H_0 [kJ/kg]	S_0 [kJ/kg.K]
1	305.15	7.5	362.2	1.531
2	376.65	26.25	408	1.555
3	540.05	26.25	672.8	2.148
4	803.15	26.25	1006	2.652
5	665.35	7.5	859	2.691
6	431.65	7.5	594.3	2.913

Table 5
Stream properties in the heat exchanger exhaust MFR of 50 kg/s, effectiveness of 0.80 and exhaust temperature of 550 °C.

T_Wh_1 [°C]	**550**
T_Wh_2 [°C]	286.9
T_Wh_3 [°C]	150
T_Wh_4 [°C]	85.74

Table 6
Comparison between the results of present study and previous work [41] *on the AC system for* $\dot{m}_{Li-Br} = 1kg/s$, $T_{Generator} = 87.8°C$, $T_{Absorber} = T_{Condenser} = 38°C$, $\varepsilon_{HE} = 0.70$ *and* $T_{Evaporator} = 7.2°C$.

Components	**Previous work by Kaushik and Arora** [41]	**Present Study**	**Unit**	**Difference(%)**
Generator	3095.7	3048	[kW]	1.56
Absorber	2945.27	2926	[kW]	0.66
Condenser	2505.91	2477	[kW]	1.17
Evaporator	2355.45	2355	[kW]	0.02
Exchanger	518.72	542	[kW]	4.29
Pump	0.0314	0.03212	[kW]	2.24
COP	0.7609	0.7726	[−]	1.51

4. Validation

To assess the applied model and validate it, two main subsystems, namely the AC and S–CO2, are separately modeled, and the obtained results are compared with the previous works by other authors. The determined values for different parameters in the present study and previous work are represented and compared in Table 6. As can be seen, the results have good agreement, and the differences between the determined value by the applied model in the present work and the data in the previous study are negligible. Table 7 compares the results obtained by the present model with the data presented in a study by Martinez et al. [40]. It can be seen that for the same conditions, there is good agreement between the results, and it can be expressed that the applied model in the present work can be properly validated.

5. Results and discussion

In this work, the effect of three factors, including the MFR of EG, the effectiveness of heat exchanger and EG temperature, on the output of the system, is investigated. In Fig. 3-a, effect of MFR on power, heating is depicted and its effect on efficiency of S–CO_2 and overall efficiency of the CCHP is illustrated in Fig. 3-b. In all of the cases, produced cooling is equal to 2356 kW. It can be seen that by elevation in the MFR, supplied heating and output power of the system increment while the cooling is constant since the MFR of AC working fluid and its input and operating condition are constant. Despite the augmentation of power and heating due to the increment of mass flow, which means higher available input for the heat recovery unit and S–CO_2 cycle, the efficiency of the CCHP is decremented, and the efficiency of the S–CO_2 cycle is constant regarding the considered assumptions (constant efficiencies of the components). By increasing the EG MFR from 30 kg/s to 50 kg/s, the efficiency of CCHP decrements from 58.63% to 56.19% for the condition of $T_{wh1} = 550°C$, effectiveness $= 0.80$, $\Delta T_{Pinch} = 20°C$, $\Delta T_{Pinch,HRU} = 30°C$ and CPR $= 3.5$. It can be attributed to the fact that the summation of produced energy in the form of heating and power by an increase in the MFR of gases is lower than the supplied energy since the efficiency of the components is lower than 1.

In addition to the MFR, the influence of exhaust gas temperature on the outputs of the system is investigated and taken into account. As shown in Fig. 4-a, in the condition of $\dot{m}_{Exhaust} = 50$ kg/s, effectiveness $= 0.80$, $\Delta T_{Pinch} = 20°C$, $\Delta T_{Pinch,HRU} = 30°C$ and CPR $= 3.5$, increment in the temperature causes augmentation in both heating and power generation regarding the higher available input energy. It should be noted that by increment in the temperature from 490 °C to 610 °C, generated power increases from 2918 kW to 3845 kW and supplied heating increases from 4814 kW to 8414 kW which is more significant from the power. Similar to the previous condition, increment in the temperature of EG causes a reduction in the efficiency of the CCHP cycle while the efficiency of the –CO_2 cycle is

Table 7
Comparison between the values of the present model and previous work [40] for simple recuperated S–CO_2 cycle by considering the same conditions (Compressor inlet pressure = 73.5 bar, compressor inlet pressure = 32 °C, compressor outlet pressure = 250 bar, recuperator effectiveness = 965%, turbine inlet pressure = 250 bar, turbine inlet temperature = 560 °C, turbine/compressor efficiency 93/89% and cycle pressure drops = 0).

Parameter	Previous work by Martinez et al. [40]	Present study	Unit	Difference (%)
Stack Temperature	343.7	339.2	[°C]	1.33
Power	25143	25067	[kW]	0.30
Cycle Efficiency	40.81	40.12	[−]	1.72
Net Work	116.6	115.92	[kW]	0.59

constant, shown in Fig. 4-b. By increment in the temperature of EG from 490 °C to 610 °C, efficiency of the CCHP decreases from 58.63% to 56.19%.

Another factor that is investigated in this study is the effectiveness of the heat exchanger used in the S–CO_2 cycle for reheating CO_2 before entering the primary heat exchanger. As illustrated in Fig. 5-a, an increase in the effectiveness from 0.7 to 0.9 induces an increment in the heating from 5395 kW to 7776 W. In this condition, the generated power slightly increases from 3377 kW to 3410 kW. These increments can be attributed to augmentation in the heat transfer between the streams in the heat exchanger that causes more available energy for the cycles. As illustrated in Fig. 5-b, the efficiency of S–CO_2 and CCHP cycles increases from 27.18% to 33.17% and 51.62%–62.47%, respectively, by increments in effectiveness from 0.7 to 0.9.

Table 8 represents shares of heating, cooling and power for different MFRs of EG at constant temperature of gases and effectiveness

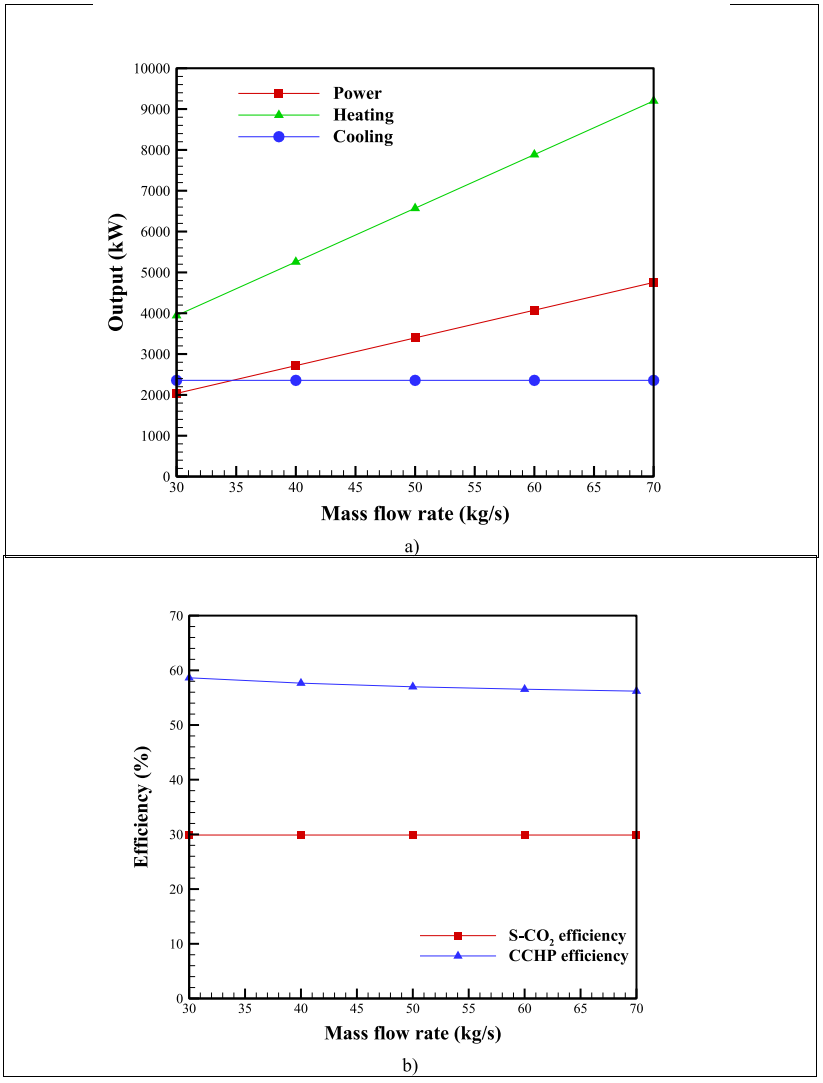

Fig. 3. Effect of MFR on a) output and b) efficiency ($T_{wh1} = 550°C, effectiveness = 0.80, \Delta T_{Pinch} = 20°C, \Delta T_{Pinch,HRU} = 30°C, CPR = 3.5$).

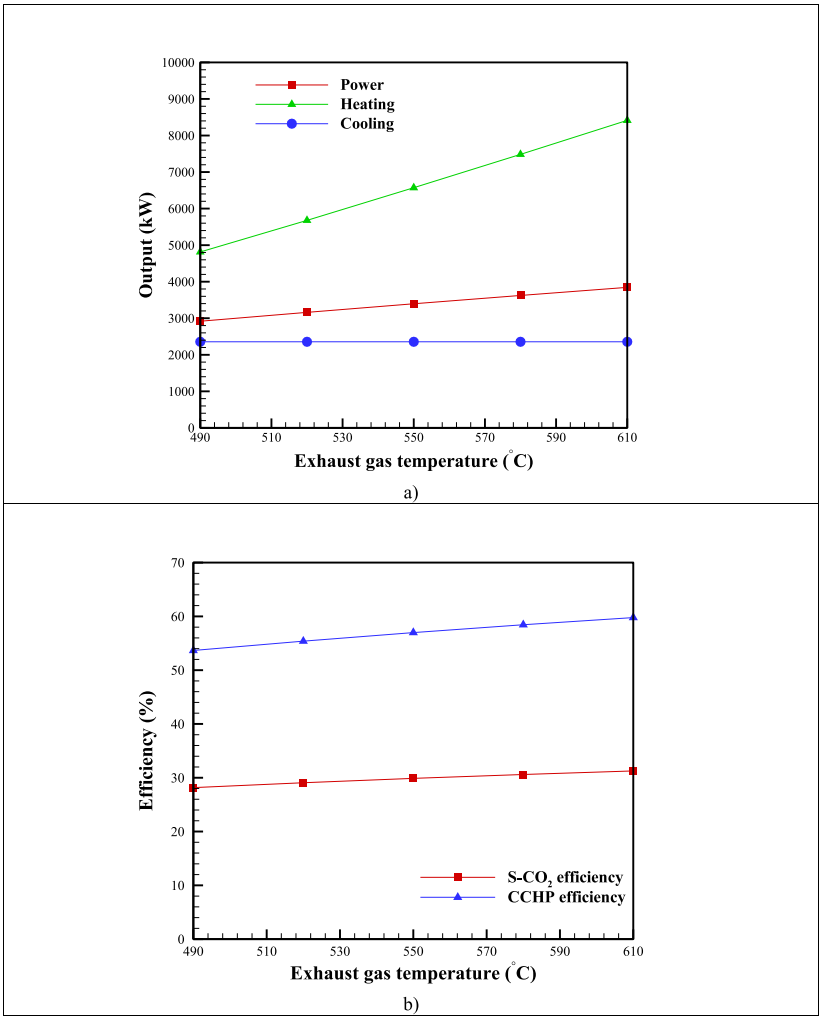

Fig. 4. Effect of exhaust gas temperature on the a) output and b) efficiency of the system ($\dot{m}_{Exhaust} = 50\ kg/s, effectiveness = 0.80, \Delta T_{Pinch} = 20°C$, $\Delta T_{Pinch,HRU} = 30°C$ *and CPR* $= 3.5$).

(see Table 7). It can be observed that with an increment in the MFR, shares of heating and power increase while the cooling share decreases. It can be attributed to the higher supplied energy to the system by increasing its MFR and constant cooling rate due to its design and assumptions. Similarly, as represented in Table 9, an increment in the gas temperature at continued effectiveness and temperature of EG causes a decrement in the share of cooling and power while causing an increase in the share of heating. It can be attributed to the higher provision of heating due to the increase in the temperature of EG, which is more noticeable than the increase in the generated power. In Table 10, effect of effectiveness on the shares of different output at constant MFR and temperature of EG is represented. It can be seen that by increment in the effectiveness, the heating share increases while the cooling and power shares decrease. It can be attributed to the higher increase rate of heating compared to power with augmentation in the effectiveness of the heat exchanger. To sum up, it can be stated that improvement in the recovered heat using increment in the temperature or MFR of EG or elevation in the effectiveness of heat exchanger induces an increase in the share of heating in the products of the proposed system while the share of cooling would be decreased owing to the design assumptions that the cooling amount would be constant regardless of the recovered heat value.

Aside from energy analysis, exergy evaluation is performed on the system's performance. As shown in Fig. 6, an increase in the MFR of EG causes a small reduction in the exergy efficiency of the system. By incrementing the MFR from 30 kg/s to 70 kg/s, exergy efficiency decreases from around 36.3% to approximately 35.1%. In Fig. 7, the impact of exhaust gas temperature on the proposed system's exergy efficiency is illustrated. It can be seen that there is approximately a linear reduction in the exergy efficiency with elevation of exhaust temperature. It can be attributed to less increment in the exergy of the product compared with the exergy of fuel, the exergy supplied to the system by EG, with an increase in the MFR or temperature of EG. The impact of heat exchanger effectiveness on the exergy efficiency is presented in Fig. 8. It is noticed that with elevation in the effectiveness, exergy efficiency of the system would be increased, mainly due to the increase in heating exergy. In this condition, by increasing the effectiveness, ED in the heat

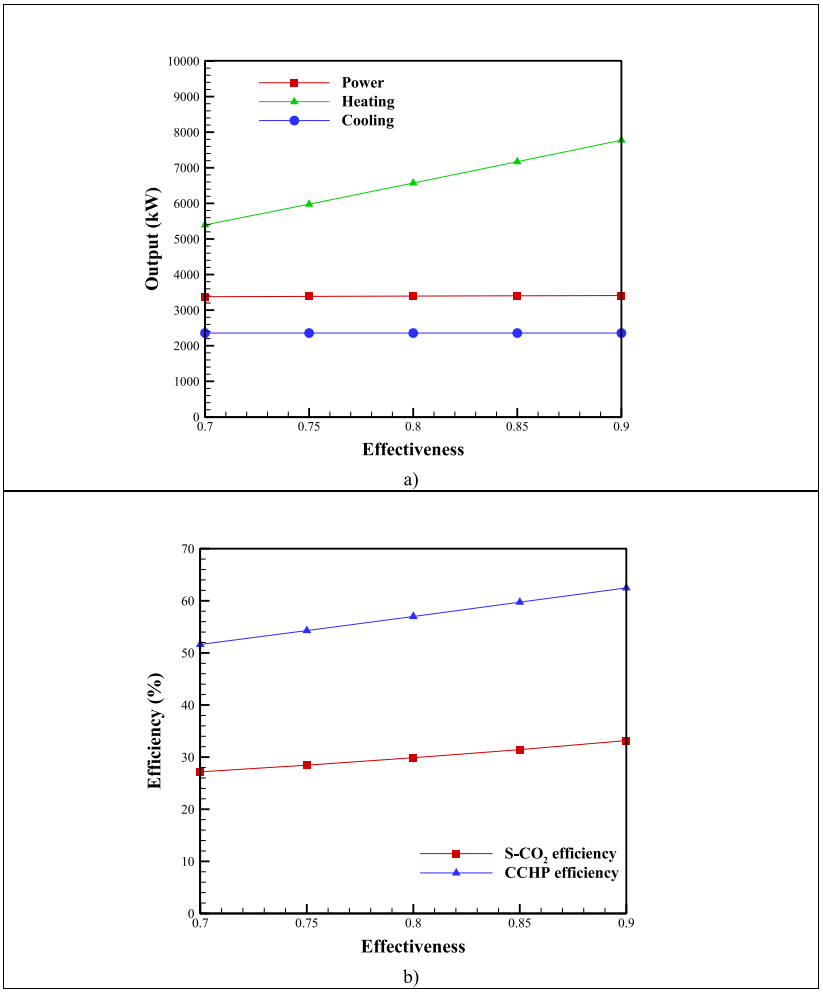

Fig. 5. Effect of heat exchanger effectiveness on a) output and b) efficiency of the system ($\dot{m}_{Exhaust} = 50\frac{kg}{s}$, $T_{wh1} = 550°C$, $\Delta T_{Pinch} = 20°C$, $\Delta T_{Pinch,HRU} = 30°C$ *and* $CPR = 3.5$).

Table 8
Shares of heating, cooling and power in the outputs of the system for T_wh1 = 550 °C, effectiveness = 0.80 and a) m˙_Exhaust = 30 kg/s, b) m˙_Exhaust = 40 kg/s, c) m˙_Exhaust = 50 kg/s, d) m˙_Exhaust = 60 kg/s, and e) m˙_Exhaust = 70 kg/s.

Case	Heating share (%)	Cooling share (%)	Power share (%)
a	47	28	25
b	51	23	26
c	51	23	26
d	55	16	29
e	56	15	29

Table 9
Shares of heating, cooling and power in the outputs of the system for effectiveness = 0.80, m˙_Exhaust = 50 kg/s and a) T_wh1 = 490 °C, b) T_wh1 = 520 °C, c) T_wh1 = 550 °C, d) T_wh1 = 580 °C, e) T_wh1 = 610 °C.

Case	Heating share (%)	Cooling share (%)	Power share (%)
a	48	23	29
b	51	21	28
c	53	19	28
d	56	17	27
e	58	16	26

Table 10
Shares of heating, cooling and power in the outputs of the system for T_wh1 = 550 °C, $\dot{m}$_Exhaust = 50 kg/s and a) effectiveness = 0.70, b) effectiveness = 0.75, c) effectiveness = 0.80, d) effectiveness = 0.85 and e) effectiveness = 0.90

Case	Heating share (%)	Cooling share (%)	Power share (%)
a	49	21	30
b	51	20	29
c	53	19	28
d	53	19	28
e	56	18	26

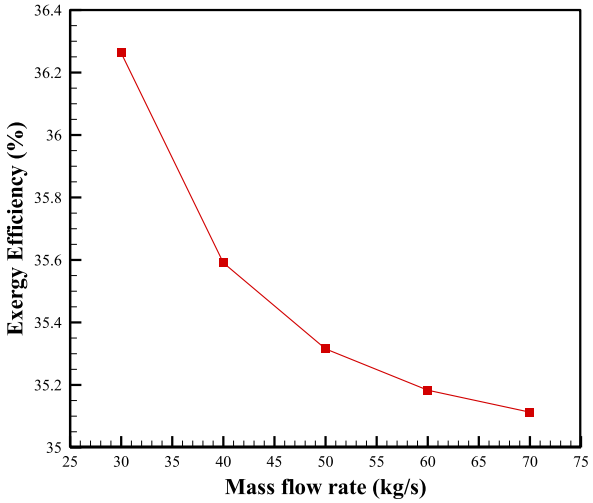

Fig. 6. Effect of EG MFR on the exergy efficiency for T_wh1 = 550 °C and effectiveness = 0.80.

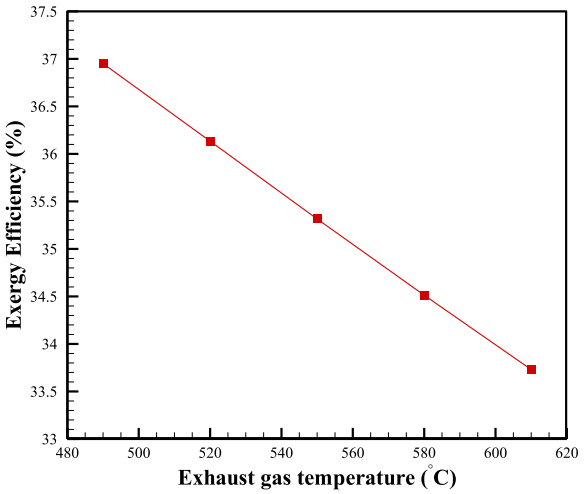

Fig. 7. Effect of temperature of EG on the exergy efficiency for effectiveness = 0.80 and $\dot{m}$_Exhaust = 50 kg/s.

exchanger would be decreased, and higher exergy efficiency would be achieved.

6. Sensitivity analysis

To calculate the importance of the factors considered in the previous section on the power and heating of the system, sensitivity analysis is implemented. Three variables, including effectiveness, MFR and temperature of the EG, are considered for the sensitivity analysis. This procedure is implemented by calculating the dependency factor that is between −1 and 1. By comparing the absolute

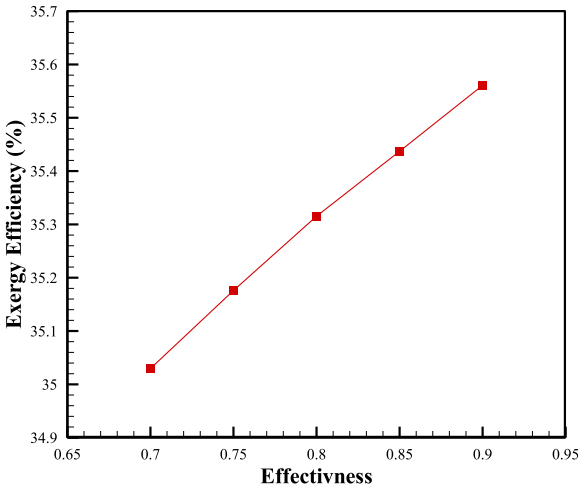

Fig. 8. Effect of heat exchanger effectiveness on the exergy efficiency for T_wh1 = 550 °C and $\dot{m}$_Exhaust = 50 kg/s.

value of the dependency factor, their importance is obtained, and higher values reveal more influence on the output. Being positive and negative for the obtained values refers to the increase and decrease of output as the result of augmentation of the associated factor. The relevancy factor of the parameters is determined as follows [1,42]:

$$r = \frac{\sum_{i=1}^{N}\left(X_{k,i} - \overline{X}_k\right)\left(y_i - \overline{y}\right)}{\sqrt{\sum_{i=1}^{N}\left(X_{k,i} - \overline{X}_k\right)^2 \sum_{i=1}^{N}\left(y_i - \overline{y}\right)^2}} \tag{55}$$

In the above equation, $\overline{y}$ refers to the output mean quantity and y_i is the quantity of ith output. $\overline{X}_k$ refers to the mean value of the kth input and *subscript refers* to the kth input quantity. In this section, the sensitivity of the power and heating of the considered system to the effectiveness, temperature and flow rate of EG are determined. As shown in Fig. 9-a and Fig. 9-b, the most influential factor on both generated power and supplied heat, respectively, is the MFR of the EG. The effectiveness of a heat exchanger is more significant than the temperature of EG for the supplied heat, while it is less important for the generated power.

Despite the technical feasibility of the proposed system in the simultaneous provision of cooling, heating and power by use of recovered thermal energy from the hot gases, there are some limitations in the use of this system. For instance, it is necessary to have a minimum input to the systems provided by the EG to have three products; therefore, there are lower limits for the MFR and temperature of the gases. Furthermore, it is crucial to apply heat exchanger with proper efficiency. Low efficiencies, values lower than 70%, can lead to remarkable decrement in the cycle performance. There would be similar degradation in the performance in conditions of high losses in the pressure lines and heat exchangers.

7. Conclusion

In this article, the performance of a CCHP system, composed of heat exchangers, absorption chiller and S–CO_2 cycle, utilizing exhaust gases of a smelting furnace is investigated by considering the effect of mass flow rate and temperature of hot gases and the effectiveness of the heat exchanger. The most important findings are as follows.

- The proposed system can generate power and supply heating and cooling with remarkable efficiency, up to 62.47%.
- Increment in the exhaust gases mass flow rate and temperature induces elevation in the generated power while the increase in the effectiveness of the heat exchanger causes a slight reduction in the generated power.
- Supplied heating increases with increments in the temperature and mass flow rate of hot gases and improvement in the effectiveness of the heat exchanger.
- The overall efficiency of the CCHP increases with increments in effectiveness while it reduces with increases in the mass flow rate and temperature of hot gases.
- Among the considered variables, namely mass flow rate and, temperature of gases and effectiveness of the heat exchanger, effect of mass flow rate is more significant on both power and heating.
- The exergy efficiency of the proposed system would be decreased with an increment in the temperature or mass flow rate of exhaust gases, while the increase in the effectiveness would lead to higher exergy efficiency.
- The importance level of effectiveness is more than the temperature of hot gases for the supplied heating, while in the case of power, the temperature of gases has more impact.

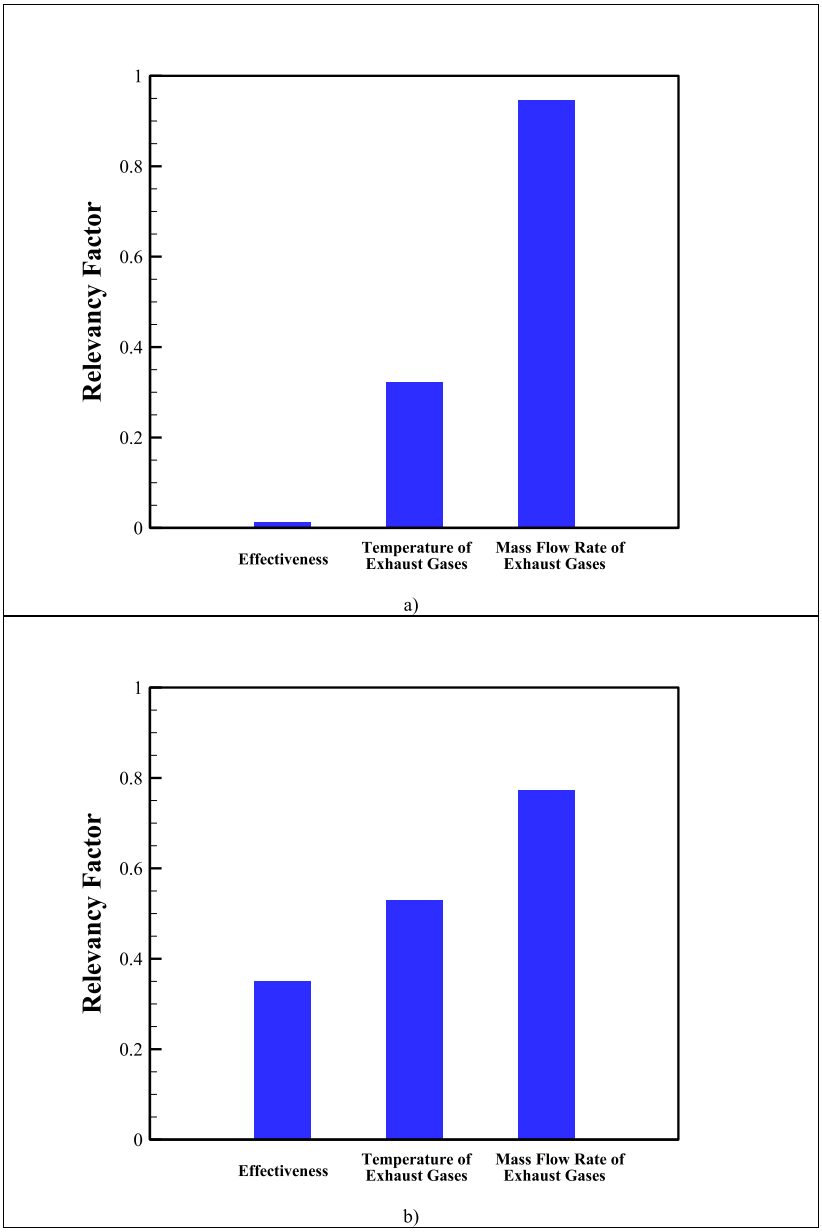

Fig. 9. Determined relevancy factor for a) generated power and b) supplied heating.

CRediT authorship contribution statement

Sina Hassanlue: Writing – original draft, Data curation, Conceptualization. **Azfarizal Mukhtar:** Writing – original draft, Validation. **Ahmad Shah Hizam Md Yasir:** Data curation, Conceptualization. **Sayed M. Eldin:** Writing – original draft, Data curation. **Mohammad A. Nazari:** Writing – original draft. **Mohammad Hossein Ahmadi:** Writing – review & editing, Supervision. **Mohsen Sharifpur:** Writing – review & editing, Supervision.

Declaration of competing interest

The authors declare that they have no known competing financial interests or personal relationships that could have appeared to influence the work reported in this paper.

References

[1] M. Sharifpur, M.H. Ahmadi, J. Rungamornrat, F.M. Mohsen, Thermal management of solar photovoltaic cell using single walled carbon nanotube (SWCNT)/Water: numerical simulation and sensitivity analysis, Sustainability 14 (2022) 11523, https://doi.org/10.3390/SU141811523, 2022;14:11523.

[2] T.E. Amin, G. Roghayeh, R. Fatemeh, P. Fatollah, Evaluation of nanoparticle shape effect on a nanofluid based flat-plate solar collector efficiency, Energy Explor. Exploit. 33 (2015) 659–676, https://doi.org/10.1260/0144-5987.33.5.659.

[3] L. Liu, Y. Tang, D. Liu, Investigation of future low-carbon and zero-carbon fuels for marine engines from the view of thermal efficiency, Energy Rep. 8 (2022) 6150–6160, https://doi.org/10.1016/j.egyr.2022.04.058.

[4] D. Gewald, K. Siokos, S. Karellas, H. Spliethoff, Waste heat recovery from a landfill gas-fired power plant, Renew. Sustain. Energy Rev. 16 (2012) 1779–1789, https://doi.org/10.1016/j.rser.2012.01.036.

[5] B. Orr, A. Akbarzadeh, M. Mochizuki, R. Singh, A review of car waste heat recovery systems utilising thermoelectric generators and heat pipes, Appl. Therm. Eng. 101 (2016) 490–495, https://doi.org/10.1016/j.applthermaleng.2015.10.081.

[6] H. Tian, R. Li, B. Salah, P.H. Thinh, Bi-objective optimization and environmental assessment of SOFC-based cogeneration system: performance evaluation with various organic fluids, Process Saf. Environ. Protect. 178 (2023) 311–330, https://doi.org/10.1016/j.psep.2023.07.040.

[7] X. Meng, R.O. Suzuki, Helical configuration for thermoelectric generation, Appl. Therm. Eng. 99 (2016) 352–357, https://doi.org/10.1016/j.applthermaleng.2016.01.061.

[8] T. Xiao, Z. Lin, C. Liu, L. Liu, Q. Li, Integration of desalination and energy conversion in a thermo-osmotic system using low-grade heat: performance analysis and techno-economic evaluation, Appl. Therm. Eng. 223 (2023) 120039, https://doi.org/10.1016/j.applthermaleng.2023.120039.

[9] C. Wang, B. He, S. Sun, Y. Wu, N. Yan, L. Yan, et al., Application of a low pressure economizer for waste heat recovery from the exhaust flue gas in a 600 MW power plant, Energy 48 (2012) 196–202, https://doi.org/10.1016/J.ENERGY.2012.01.045.

[10] B. Orr, A. Akbarzadeh, Prospects of waste heat recovery and power generation using thermoelectric generators, Energy Proc 110 (2017) 250–255, https://doi.org/10.1016/J.EGYPRO.2017.03.135.

[11] Z.Y. Xu, H.C. Mao, D.S. Liu, R.Z. Wang, Waste heat recovery of power plant with large scale serial absorption heat pumps, Energy 165 (2018) 1097–1105, https://doi.org/10.1016/J.ENERGY.2018.10.052.

[12] G.V. Pradeep Varma, T. Srinivas, Design and analysis of a cogeneration plant using heat recovery of a cement factory, Case Stud. Therm. Eng. 5 (2015) 24–31, https://doi.org/10.1016/j.csite.2014.12.002.

[13] A. Naeimi, M. Bidi, M.H. Ahmadi, R. Kumar, M. Sadeghzadeh, M. Alhuyi Nazari, Design and exergy analysis of waste heat recovery system and gas engine for power generation in Tehran cement factory, Therm. Sci. Eng. Prog. 9 (2019) 299–307, https://doi.org/10.1016/j.tsep.2018.12.007.

[14] H. Chen, Y. Wang, L. An, G. Xu, X. Zhu, W. Liu, et al., Performance evaluation of a novel design for the waste heat recovery of a cement plant incorporating a coal-fired power plant, Energy 246 (2022) 123420, https://doi.org/10.1016/J.ENERGY.2022.123420.

[15] M.R. Gomaa, T.K. Murtadha, A. Abu-jrai, H. Rezk, M.A. Altarawneh, A. Marashli, Experimental investigation on waste heat recovery from a cement factory to enhance thermoelectric generation, Sustainability 14 (2022) 10146, https://doi.org/10.3390/SU141610146, 2022;14:10146.

[16] D. Brough, H. Jouhara, The aluminium industry: a review on state-of-the-art technologies, environmental impacts and possibilities for waste heat recovery, International Journal of Thermofluids 1–2 (2020) 100007, https://doi.org/10.1016/j.ijft.2019.100007.

[17] Y. Liu, Y. Wang, D. Huang, Supercritical CO2 Brayton cycle: a state-of-the-art review, Energy 189 (2019) 115900, https://doi.org/10.1016/J.ENERGY.2019.115900.

[18] H. Chen, M. Zhang, Y. Wu, G. Xu, W. Liu, T. Liu, Design and performance evaluation of a new waste incineration power system integrated with a supercritical CO2 power cycle and a coal-fired power plant, Energy Convers. Manag. 210 (2020) 112715, https://doi.org/10.1016/J.ENCONMAN.2020.112715.

[19] G. Manente, F.M. Fortuna, Supercritical CO2 power cycles for waste heat recovery: a systematic comparison between traditional and novel layouts with dual expansion, Energy Convers. Manag. 197 (2019) 111777, https://doi.org/10.1016/J.ENCONMAN.2019.111777.

[20] O. Olumayegun, M. Wang, Dynamic modelling and control of supercritical CO2 power cycle using waste heat from industrial processes, Fuel 249 (2019) 89–102, https://doi.org/10.1016/J.FUEL.2019.03.078.

[21] J. Wang, Z. Sun, Y. Dai, S. Ma, Parametric optimization design for supercritical CO2 power cycle using genetic algorithm and artificial neural network, Appl. Energy 87 (2010) 1317–1324, https://doi.org/10.1016/J.APENERGY.2009.07.017.

[22] D. Novales, A. Erkoreka, V. De la Peña, B. Herrazti, Sensitivity analysis of supercritical CO2 power cycle energy and exergy efficiencies regarding cycle component efficiencies for concentrating solar power, Energy Convers. Manag. 182 (2019) 430–450, https://doi.org/10.1016/J.ENCONMAN.2018.12.016.

[23] L. Sun, Y. Wang, D. Wang, Y. Xie, Parametrized analysis and multi-objective optimization of supercritical CO2 (S-CO2) power cycles coupled with parabolic trough collectors, Appl. Sci. 10 (2020) 3123, https://doi.org/10.3390/APP10093123, 2020;10:3123.

[24] M. Salimi, M. Hosseinpour, S. Mansouri, T.N. Borhani, Environmental aspects of the combined cooling, heating, and power (CCHP) systems: a review, Processes 10 (2022) 711, https://doi.org/10.3390/PR10040711, 2022;10:711.

[25] M. Ebrahimi, A. Keshavarz, CCHP technology. Combined cooling, Heating and Power 35–91 (2015), https://doi.org/10.1016/B978-0-08-099985-2.00002-0.

[26] T. Ai, H. Chen, J. Jia, Y. Song, F. Zhong, S. Yang, et al., Thermodynamic analysis of a CCHP system integrated with a regenerative organic flash cycle, Appl. Therm. Eng. 202 (2022) 117833, https://doi.org/10.1016/j.applthermaleng.2021.117833.

[27] S. Wang, L. Zhang, C. Liu, Z. Liu, S. Lan, Q. Li, et al., Techno-economic-environmental evaluation of a combined cooling heating and power system for gas turbine waste heat recovery, Energy 231 (2021) 120956, https://doi.org/10.1016/j.energy.2021.120956.

[28] S. Wang, C. Liu, J. Li, Z. Sun, X. Chen, X. Wang, Exergoeconomic analysis of a novel trigeneration system containing supercritical CO2 Brayton cycle, organic Rankine cycle and absorption refrigeration cycle for gas turbine waste heat recovery, Energy Convers. Manag. 221 (2020) 113064, https://doi.org/10.1016/j.enconman.2020.113064.

[29] A. Wang, S. Wang, A. Ebrahimi-Moghadam, M. Farzaneh-Gord, A.J. Moghadam, Techno-economic and techno-environmental assessment and multi-objective optimization of a new CCHP system based on waste heat recovery from regenerative Brayton cycle, Energy 241 (2022) 122521, https://doi.org/10.1016/j.energy.2021.122521.

[30] A. Ahmed, K.K. Esmaeil, M.A. Irfan, F.A. Al-Mufadi, Design methodology of organic Rankine cycle for waste heat recovery in cement plants, Appl. Therm. Eng. 129 (2018) 421–430, https://doi.org/10.1016/j.applthermaleng.2017.10.019.

[31] E.P.B. Júnior, M.D.P. Arrieta, F.R.P. Arrieta, C.H.F. Silva, Assessment of a Kalina cycle for waste heat recovery in the cement industry, Appl. Therm. Eng. 147 (2019) 421–437, https://doi.org/10.1016/J.APPLTHERMALENG.2018.10.088.

[32] A. Redko, O. Redko, R. DiPippo, Industrial Waste Heat Resources, Academic Press, Cambridge, MA, 2020, pp. 329–362.

[33] M.A. Ancona, M. Bianchi, L. Branchini, A. De Pascale, F. Melino, A. Peretto, et al., Systematic comparison of ORC and s-CO2 combined heat and power plants for energy harvesting in industrial gas turbines, Energies 14 (2021) 3402, https://doi.org/10.3390/en14123402.

[34] M. Mirzaei, M.H. Ahmadi, M. Mobin, M.A. Nazari, R. Alayi, Energy, exergy and economics analysis of an ORC working with several fluids and utilizes smelting furnace gases as heat source, Therm. Sci. Eng. Prog. 5 (2018) 230–237, https://doi.org/10.1016/j.tsep.2017.11.011.

[35] M. Marchionni, G. Bianchi, S.A. Tassou, Review of supercritical carbon dioxide (sCO2) technologies for high-grade waste heat to power conversion, SN Appl. Sci. 2 (2020) 1–13, https://doi.org/10.1007/s42452-020-2116-6.

[36] S.J. Hoque, P. Kumar, Analysis of a dual recuperated dual expansion supercritical CO2 cycle for waste heat recovery applications, Transactions of the Indian National Academy of Engineering 6 (2021) 439–459, https://doi.org/10.1007/s41403-021-00211-4.

[37] V. Kunniyoor, P. Singh, K. Nadella, Value of closed-cycle gas turbines with design assessment, Appl. Energy 269 (2020) 114950, https://doi.org/10.1016/j.apenergy.2020.114950.

[38] H. Ke, S.K. R R, Absorption Chillers and Heat Pumps, CRC Press, Boca Raton (FL), 1996.

[39] R. Touaibi, M. Feidt, E.E. Vasilescu, M.T. Abbes, Parametric study and exergy analysis of solar water-lithium bromide absorption cooling system, Int. J. Exergy 13 (2013) 409–429, https://doi.org/10.1504/IJEX.2013.057358.

[40] Martínez G, Sánchez D, … FC-P of the 1st, 2017 Undefined. A Global Approach to Assessing the Potential of Combined Cycles Using Supercritical Technology. GppsGlobal n.d..

[41] S.C. Kaushik, A. Arora, Energy and exergy analysis of single effect and series flow double effect water-lithium bromide absorption refrigeration systems, Int. J. Refrig. 32 (2009) 1247–1258, https://doi.org/10.1016/j.ijrefrig.2009.01.017.

[42] A. Baghban, M. Kahani, M.A. Nazari, M.H. Ahmadi, W.-M. Yan, Sensitivity analysis and application of machine learning methods to predict the heat transfer performance of CNT/water nanofluid flows through coils, Int. J. Heat Mass Tran. 128 (2019) 825–835, https://doi.org/10.1016/J.IJHEATMASSTRANSFER.2018.09.041.